ISSN 0304-9892 (Print) ISSN 2455-7463 (Online)
www.vijnanaparishadofindia.org/jnanabha

Jñānābha, **Vol. 56(1) (2026), 159-169**

HALL CURRENT AND VISCOUS DISSIPATION ON *MHD* NATURAL CONVECTION FLOW WITH THERMAL STRATIFICATION

Nidhi Pandya and Shikha Rawat
Department of Mathematics and Astronomy, University of Lucknow, Lucknow, Uttar Pradesh, India-226007
Email: dr.nidh23@gmail.com, rawatshikha05@gmail.com
(Received: March 25, 2025*; In format: May* 07, 2026*; Revised: June* 08, 2026*; Accepted: June* 27, 2026*)*

DOI: https://doi.org/10.58250/jnanabha.2026.56116

Abstract

The study's unsteady *MHD* free convective flow traverses a porous material that is influenced by thermal radiation, heat absorption, the hall effect and thermal stratification as it passes over a vertically inclined temperature-varying flat plate. The governing equations are transformed into a dimensionless form by applying the appropriate transformation and solved by using Crank-Nicolson method, numerically. The graphical results have been achieved using Mathematica. The results demonstrate that radiation and heat absorption have a significant effect on the velocity and temperature profiles on thermally stratified fluid.
2020 Mathematical Sciences Classification: 76W05, 76D10, 76S05, 80A20, 65M06.
Keywords and Phrases: MHD, Thermally stratification, Viscous dissipation, Hall current, Crank-Nicolson method.

Nomenclature

B_0 Strength of magnetic field
u' Dimensional velocity of plate in x-direction
v' Dimensional velocity of plate in y-direction
w' Dimensional velocity of plate in z-direction
T' Dimensional Fluid temperature
u Dimensionless velocity
g Gravitational acceleration
β_T Coefficient of thermal expansion
α angle of inclination
σ Electrical conductivity
σ_s Stefan-Boltzmann Constant
ρ Fluid density
ν Kinematic viscosity
K' Dimensional permeability of porous medium
κ Thermal conductivity
k_e mean absorption coefficient
C_p Specific heat at constant pressure
μ viscosity of the fluid
q_r Radiative heat flux
Q_0 heat absorption coefficient
T_∞ Fluid temperature far away from the plate
T_w wall temperature
A Constant buoyancy frequency
Gr Thermal Grashof number
θ Non-dimensional temperature
M Magnetic parameter
Pr Prandtl number
R Radiation parameter
S stratification parameter
Ec Eckert number
Q Heat absorption parameter
P Pressure
τ Skin friction
m hall parameter

1 Introduction

The importance of magnetohydrodynamic free convection stems from its presence in both natural and fluid engineering situations. One example of how free convection is used in a natural phenomenon is the ocean currents, which are caused by variations in salt and temperature difference in the layers of the water. This temperature difference between the layers of the water is known as thermal stratification, Which is applicable in energy extraction procedures from sea waves. Hall current, heat source or sinks, thermal radiation and thermal stratification all have a significant impact on the pace of heat transmission, which determines the quality of the finished product.

Many scholars have examined the dynamics of flow and heat transmission. Chakrabarti and Gupta [2] who measured the heat transfer in hydro-magnetic flow. Grubka and Bobba [7] investigated the properties of heat transfer and fluid flow on a stretching sheet at different temperatures. In a boundary layer flow through a porous media, Chaudhary *et al*[3] investigated the complexities on *MHD* and Khan *et al.*[10] worked on dissipation energy and stress work on unsteady *MHD* free convection flow of heat transfer. A porous stretching sheet in porous media with a range of effects were discussed by Vijayalakshmi *et al.*[17] and Raju *et al.*[13]. In their research on heat transport in a porous media, temperature-dependent heat sources have been taken into consideration by Moalem [11] and Chamkha [4]. Soid and Ishak [15] estimates thermal boundary layer flow over an increasingly stretched surface with radiation effect.

Recently, The effects of varied fuid characteristics and viscous dissipation on the transport phenomenon were discussed by Reddy *et al.*[14], Das *et al.*[5], Ferdows *et al.*[6] and Megahed *et al.*[12]. Researchers Barik *et al.*[1] studied the effects of thermal radiation on an unstable *MHD* flow past an inclined porous heated plate in the context of viscous dissipation, and Iranian D [9] studied the effects of varying viscosity, thermal conductivity, and stratification parameter with velocity and temperature profiles. Senge *et al.*[16] investigated the *MHD* in a thermally stratified porous medium in the presence of heat source. Goud *et al.*[8] used an accelerating perpendicular plate with *MHD* to examine the viscous dissipation-affected time-dependent thermally stratified flow through a porous medium.

In an effort to close the gap with the previously mentioned literature, the study investigated the effects of thermal stratification, radiation, viscous dissipation, and the hall effect using an unsteady *MHD* flow across a temperaturevarying vertically angled plate.

2 Mathematical Formulation

This paper considers radiation, thermal stratification, and viscous dissipation with hall effect in the context of an incompressible, unsteady, free convective viscous *MHD* flow via a semi-infinite nonconducting vertically angled plates inserted in a porous medium. In contrast to the direction of gravity, the x-axis rises vertically while the y-axis is perpendicular to the plate. Figure 2.1 depicts the problem's schematic arrangement. In the x' and y' directions, the plate is positioned after an α, tilt from the vertical x-axis. The homogeneous magnetic field, B_0, is speculated transversely to the flow direction. Hall currents are generated as a result of the strong magnetic field which ultimately result in the magnetic forces exerted on the fluid in motion. The Hall parameter $m(=\omega_e\tau_e)$ is introduced in order to account for the Hall effect, where ω_e and τ_e represent the electron frequency and electron collision time respectively. At $t' \leq 0$, the fluid and plate are initially at rest with a temperature T_∞. The plate experiences a sudden jerk after time t', which causes the fluid to flow with a velocity $A\sqrt{A\nu}t'$ and raise its temperature to T_w.

With the use of the generalized Ohm law, the conservation of electric charge equation yields the electric current density component in x and z direction as follows:

$$J'_x = \frac{\sigma B_0}{1+m^2}(mu' - w') \;, \tag{2.1}$$

$$J'_z = \frac{\sigma B_0}{1+m^2}(u' + mw') \;. \tag{2.2}$$

Here, u' and w' are the velocity and secondary velocity for the fluid flow in x' and z' direction respectively. The flow variables are only functions of y' and t' because of the infinite length in the x' direction.

Under the prior assumptions, the governing boundary layer equations using Boussinesq's approximation are

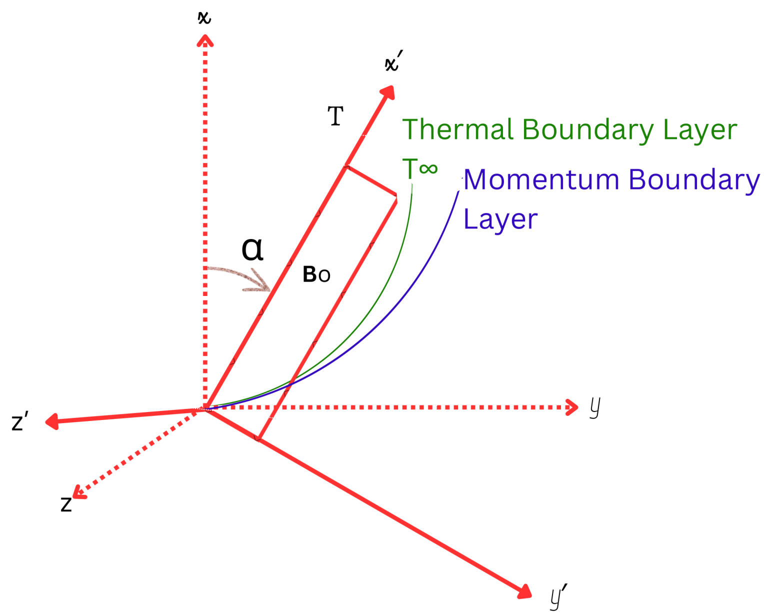

Figure 2.1: *Configuration of the physical model of the problem*

$$\frac{\partial v'}{\partial y'} = 0 \; , \tag{2.3}$$

$$\frac{\partial u'}{\partial t'} + v'\frac{\partial u'}{\partial y'} = \nu\frac{\partial^2 u'}{\partial y'^2} + g\beta_T(T' - T_\infty)cos\alpha - \frac{\sigma B_0^2}{\rho(1+m^2)}(u' + mw') - \frac{\nu}{K'}u' \tag{2.4}$$

$$\frac{\partial w'}{\partial t'} + v'\frac{\partial w'}{\partial y'} = \nu\frac{\partial^2 w'}{\partial y'^2} + \frac{\sigma B_0^2}{\rho(1+m^2)}(mu' - w') - \frac{\nu}{K'}w', \tag{2.5}$$

$$\frac{\partial T'}{\partial t'} + v'\frac{\partial T'}{\partial y'} = \frac{\kappa}{\rho C_p}\frac{\partial^2 T'}{\partial y'^2} - \gamma(u' + w') + \frac{\mu}{\rho C_p}((\frac{\partial u'}{\partial y'})^2 + (\frac{\partial w'}{\partial y'})^2) - \frac{1}{\rho Cp}\frac{\partial q_r}{\partial y'} - \frac{Q_0}{\rho C_p}(T' - T_\infty). \tag{2.6}$$

where

$$\gamma = \frac{dT_w}{dy'} + \frac{g}{C_p}.$$

In this case, pressure work is denoted by $\frac{g}{C_P}$ and thermal stratification by $\frac{dT_\infty}{dz}$. It is assumed that the fluid flow has the following initial and boundary conditions

$$u'(y',0) = 0, \;\; w'(y',0) = 0, \;\; T'(y',0) = T_\infty \;\; \forall\, y' > 0, \tag{2.7}$$

$$u'(0,t') = A\sqrt{A\nu}\, t', \;\; w'(0,t') = A\sqrt{A\nu}\, t', \;\; T'(0,t') = T_\infty + (T_w - T_\infty)e^{At'} \;\; \forall\, t' > 0, \tag{2.8}$$

$$u'(y',t') \to 0, \;\; w'(y',t') \to 0, \;\; T'(y',t') \to T_\infty \;\; as \;\; y' \to \infty. \tag{2.9}$$

Where $v' = -\sqrt{\nu A}$ be the velocity in z-drection and A $= \frac{\gamma u'}{\Delta T'}$ is given as buoyancy frequency which measures a fluid's resistance to vertical displacements like those carried on by convection. It is presumed that thermal radiation exists. The radiative heat flow, denoted by q_r, can be calculated using Rosseland's approximation.

$$q_r = -\frac{4\sigma_s}{3k_e}\frac{\partial T'^4}{\partial y'}.$$

If the flow's temperature gradients are low enough, we can get a linear version by substituting T'^4 in a Taylor series by leaving out higher order components around T_∞ as-

$$T'^4 = 4{T_\infty}^3 T' - 3{T_\infty}^4.$$

We introduce the subsequent non-dimensional quantities:

$$y = \sqrt{\frac{A}{\nu}}y', \;\; u = \frac{u'}{\sqrt{\nu A}}, \;\; w = \frac{w'}{\sqrt{\nu A}}, \;\; t = At', \;\; K = \frac{K'A}{\nu}, \;\; Gr = \frac{g\beta_T(T_w - T_\infty)}{A\sqrt{\nu A}},$$
$$\theta = \frac{T' - T_\infty}{T_w - T_\infty}, \;\; M = \frac{\sigma {B_0}^2}{\rho A}, \;\; Pr = \frac{\mu C_P}{\kappa}, \;\; \mu = \rho\nu, \;\; S = \frac{\sqrt{\nu}\,\gamma}{\sqrt{A}(T_w - T_\infty)},$$
$$Q = \frac{Q_0}{\rho C_p A}, \;\; R = \frac{k_e \kappa}{4\sigma_s {T_\infty}^3}, \;\; Ec = \frac{\nu A}{C_p(T_w - T_\infty)}.$$

Dimensionless values can be used to simplify equations (2.4) to (2.9). Therefore, equations in their non-dimensionalized form (2.4) to (2.9) convert as follows:

$$\frac{\partial u}{\partial t} - \frac{\partial u}{\partial y} = \frac{\partial^2 u}{\partial y^2} + Gr\theta cos\alpha - (\frac{M}{1+m^2} + \frac{1}{K})u - \frac{mM}{1+m^2}w, \tag{2.10}$$

$$\frac{\partial w}{\partial t} - \frac{\partial w}{\partial y} = \frac{\partial^2 w}{\partial y^2} - (\frac{M}{1+m^2} + \frac{1}{K})w + \frac{mM}{1+m^2}u, \tag{2.11}$$

$$\frac{\partial \theta}{\partial t} - \frac{\partial \theta}{\partial y} = \frac{1}{Pr}(1 + \frac{4}{3R})\frac{\partial^2 \theta}{\partial y^2} - S(u+w) + Ec((\frac{\partial u}{\partial y})^2 + (\frac{\partial w}{\partial y})^2) - Q\theta. \tag{2.12}$$

Following are the relevant non-dimensional boundary conditions:

$$u(y,0) = 0, \;\; w(y,0) = 0, \;\; \theta(y,0) = 0, \;\; \forall\, y > 0, \tag{2.13}$$
$$u(0,t) = t, \;\; w(0,t) = t, \;\; \theta(0,t) = e^t \;\; \forall\, t > 0, \tag{2.14}$$
$$u(y,t) \to 0, \;\; w(y,t) \to 0, \;\; \theta(y,t) \to 0 \;\; as \;\; y \to \infty \;\; \forall\, t > 0. \tag{2.15}$$

Equations (2.16) to (2.18) can be used to estimate the values of Skin Friction as well as Nusselt Number.

Skin Friction. Skin friction is determined by:

$$\tau_1 = (\frac{\partial u}{\partial y})_{y=0}, \tag{2.16}$$

$$\tau_2 = (\frac{\partial w}{\partial y})_{y=0}. \tag{2.17}$$

Nusselt Number Nusselt number is determined by:

$$Nu = -(\frac{\partial \theta}{\partial y})_{y=0}. \tag{2.18}$$

Solution. Set up the proper beginning and boundary conditions, then use the implicit finite difference approach of the Crank and Nicolson model to solve the non-linear momentum and energy equations (2.10) to (2.15). As such, we use the Nicolson approach to obtain the relevant finite difference equations

$$\begin{aligned}\frac{u_{i,j+1} - u_{i,j}}{\Delta t} - \frac{u_{i+1,j} - u_{i,j}}{\Delta y} &= \left(\frac{u_{i+1,j+1} - 2u_{i,j+1} + u_{i-1,j+1} + u_{i+1,j} - 2u_{i,j} + u_{i-1,j}}{2(\Delta y)^2}\right) \\ &+ Gr\cos(\alpha)\left(\frac{\theta_{i,j+1} + \theta_{i,j}}{2}\right) - \left(\frac{M}{1+m^2} + \frac{1}{K}\right)\left(\frac{u_{i,j+1} + u_{i,j}}{2}\right) \\ &- \left(\frac{mM}{1+m^2}\right)\left(\frac{w_{i,j+1} + w_{i,j}}{2}\right),\end{aligned} \tag{2.19}$$

$$\begin{aligned}\frac{w_{i,j+1} - w_{i,j}}{\Delta t} - \frac{w_{i+1,j} - w_{i,j}}{\Delta y} &= \left(\frac{w_{i+1,j+1} - 2w_{i,j+1} + w_{i-1,j+1} + w_{i+1,j} - 2w_{i,j} + w_{i-1,j}}{2(\Delta y)^2}\right) \\ &- \left(\frac{M}{1+m^2} + \frac{1}{K}\right)\left(\frac{w_{i,j+1} + w_{i,j}}{2}\right) + \left(\frac{mM}{1+m^2}\right)\left(\frac{u_{i,j+1} + u_{i,j}}{2}\right),\end{aligned} \tag{2.20}$$

$$\begin{aligned}\frac{\theta_{i,j+1} - \theta_{i,j}}{\Delta t} - \frac{\theta_{i,j+1} - \theta_{i,j}}{\Delta y} &= \frac{1}{Pr}\left(1 + \frac{4}{3R}\right)\left(\frac{\theta_{i+1,j+1} - 2\theta_{i,j+1} + \theta_{i-1,j+1} + \theta_{i+1,j} - 2\theta_{i,j} + \theta_{i-1,j}}{2(\Delta y)^2}\right) \\ &- S\left(\frac{u_{i,j+1} + u_{i,j}}{2}\right) + \left(\frac{w_{i,j+1} + w_{i,j}}{2}\right) \\ &+ Ec\left(\left(\frac{u_{i+1,j} - u_{i,j}}{\Delta y}\right)^2 + \left(\frac{w_{i+1,j} - w_{i,j}}{\Delta y}\right)^2\right) - Q\left(\frac{\theta_{i,j+1} + \theta_{i,j}}{2}\right).\end{aligned} \tag{2.21}$$

The related boundary conditions are as follows:

$$u_{i,0} = 0, \;\; w_{i,0} = 0, \;\; \theta_{i,0} = 0 \;\; \forall\, i, \tag{2.22}$$

$$u_{0,j} = j\Delta t, \;\; w_{0,j} = j\Delta t, \;\; \theta_{0,j} = e^{j\Delta t} \;\; \forall\, j > 0, \tag{2.23}$$

$$u_{L,j} \to 0, \;\; w_{L,j} \to 0, \;\; \theta_{L,j} \to 0 \;\; as \;\; L \to \infty \;\; \forall\, j > 0. \tag{2.24}$$

Here, time t is indicated by index j, while space y is shown by index i. Furthermore, accordingly, the mesh sizes along the time t-direction and the y-direction are represented by Δt and Δy. The tri-diagonal system of equations consisting of the finite difference equations (2.19) to (2.21) at each internal nodal point on a given n-level is solved using the Thomas algorithm.

3 Results and Discussion

The temperature(θ) and velocity (u and w) profiles are shown using graphs based on various flow parameter values. The graphic analysis of the effects of different parameters, such as the heat absorption parameter Q, radiation parameter (R), thermal stratification parameter (S), thermal Grashof number (Gr), Hartmann number (M), hall parameter (m), angle of inclination (α), Eckert number (Ec) and Prandtl number (Pr) on the temperature field and velocity distribution is shown in Figures 3.1 to 3.21.

When seen in Figure 3.1 and Figure 3.2, the angle of inclination (α) decreases, both u and w increases. The link of both fluid velocity u as well as w between K, Gr and m is depicted in Figures 3.2 to 3.8 as, these parameters values increase, consequently increases the fluid's velocity. Figures 3.9 and 3.10 illustrates how velocity u falls and w rise with increasing M. In Figures 3.11 and 3.12 velocity decreases in nature for increasing values of Prandtl number. In addition, velocity u increases with increasing value of Ec in Figure 3.13. Decreasing effect of Q, R and S have been seen in Figures 3.14 to 3.16 for u. Figure 3.17 illustrates how increasing the Ec causes the fluid's temperature to rise. Figures 3.18 to 3.21 shows the decreasing influence of Pr, Q, R and S on θ The temperature falls when Pr, Q, R and S rises

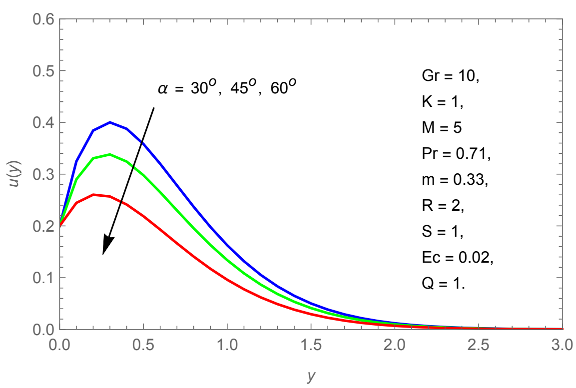

***Figure* 3.1:** *Velocity* (u) *v/s* α

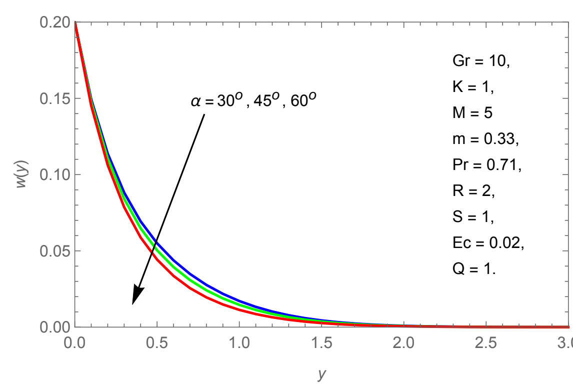

***Figure* 3.2:** *Velocity* (w) *v/s* α

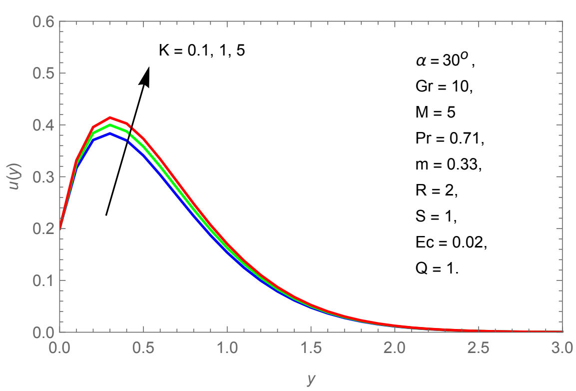

***Figure* 3.3:** *Velocity* (u) *v/s* K

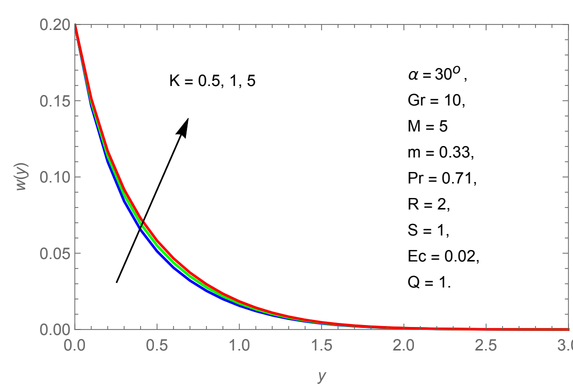

***Figure* 3.4:** *Velocity* (u) *v/s* K

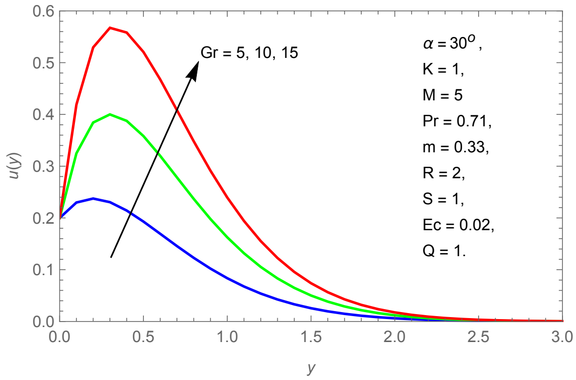

Figure 3.5: *Velocity (u) v/s Gr*

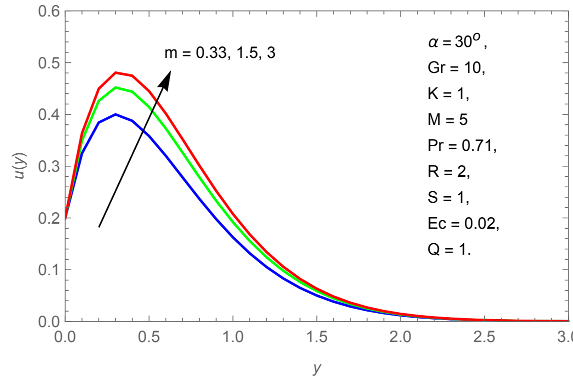

Figure 3.6: *Velocity (u) v/s m*

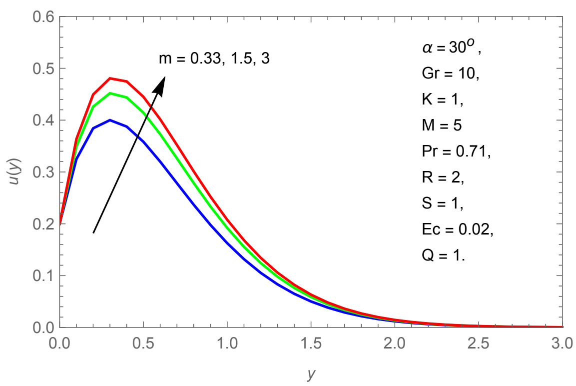

Figure 3.7: *Velocity (u) v/s m*

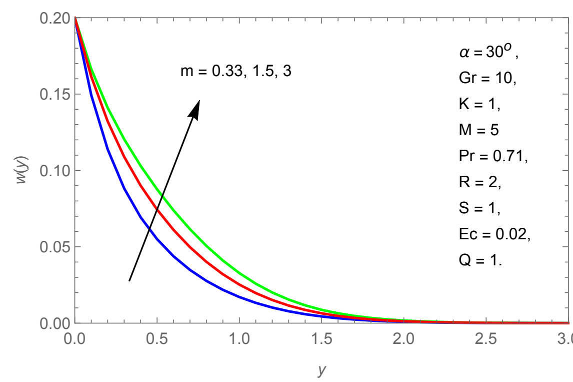

Figure 3.8: *Velocity (w) v/s m*

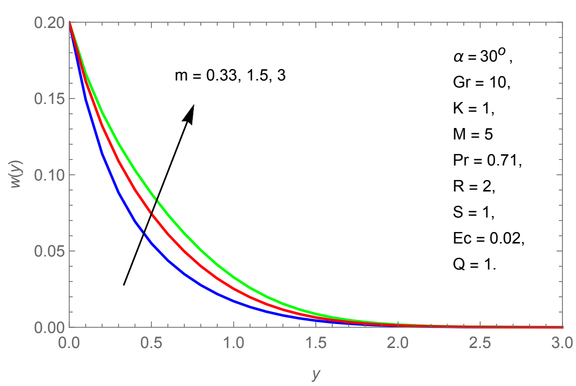

Figure 3.9: *Velocity (w) v/s m*

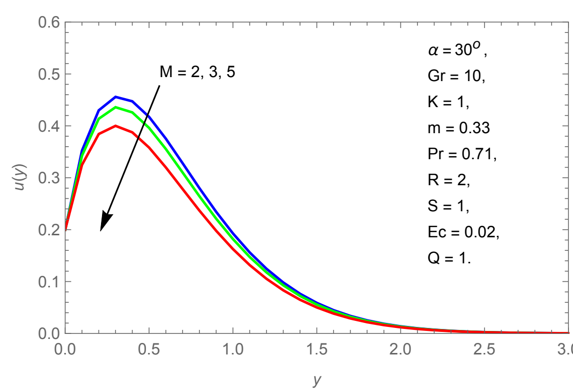

Figure 3.10: *Velocity (u) v/s M*

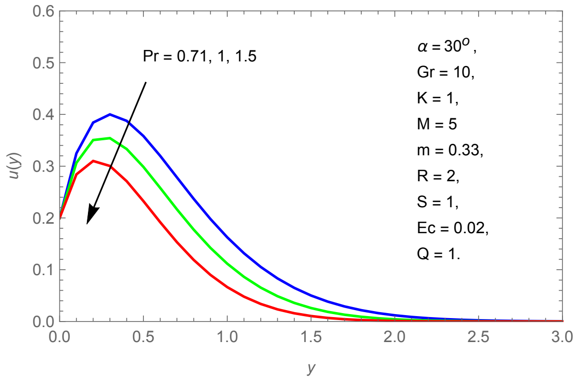

***Figure* 3.11:** *Velocity* (u) v/s Pr

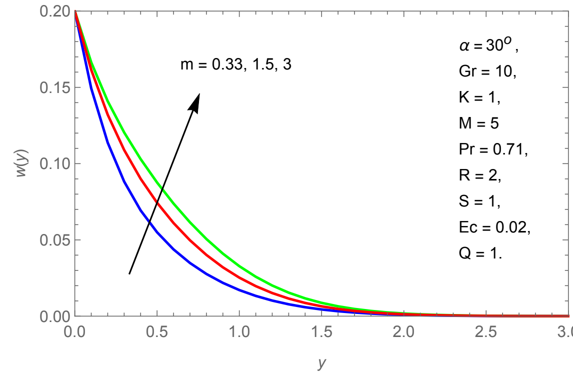

***Figure* 3.12:** *Velocity* (w) v/s m

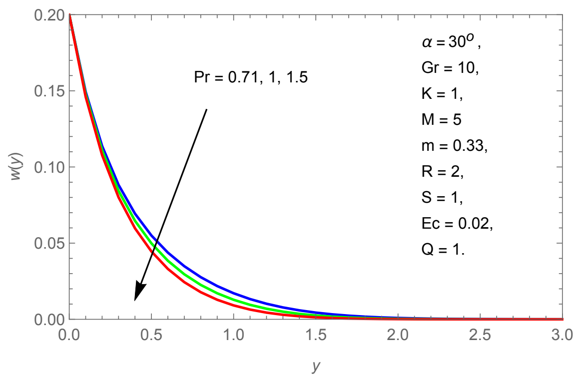

***Figure* 3.13:** *Velocity* (w) v/s Pr

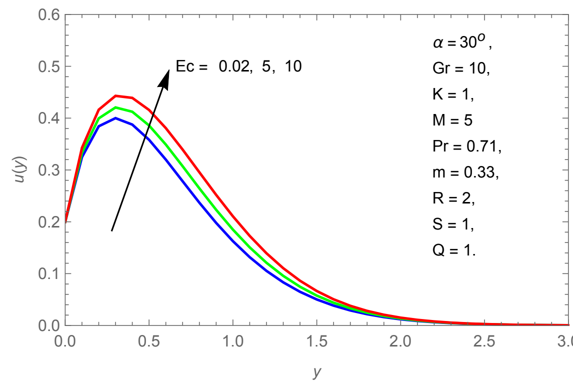

***Figure* 3.14:** *Velocity* (u) v/s Ec

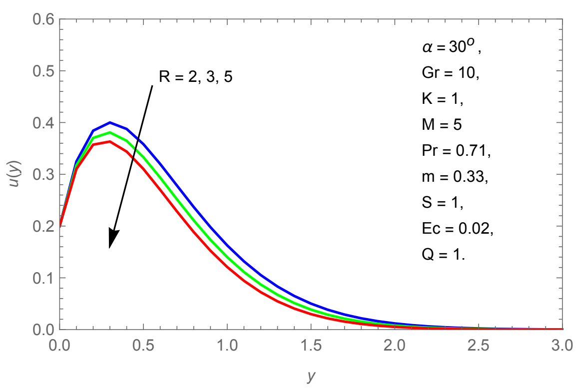

***Figure* 3.15:** *Velocity* (u) v/s R

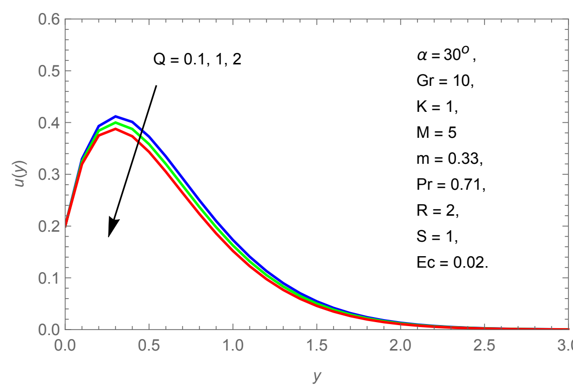

***Figure* 3.16:** *Velocity* (u) v/s Q

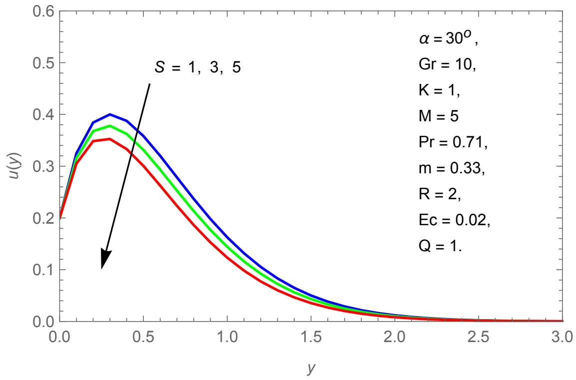

***Figure* 3.17:** *Velocity* (u) *v/s* S

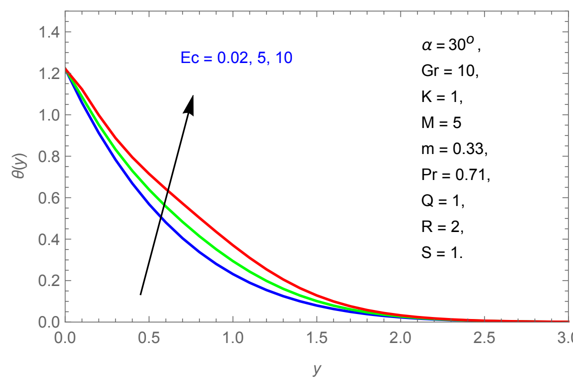

***Figure* 3.18:** *Temperature* θ *v/s* Ec

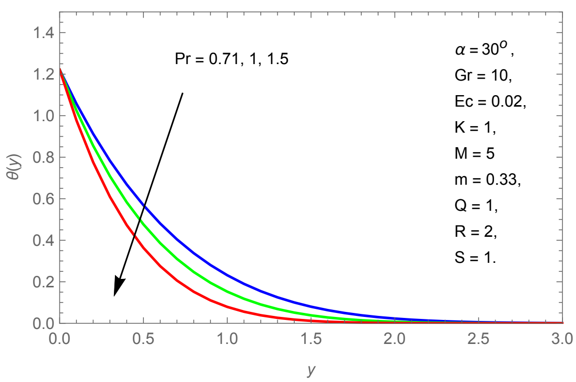

***Figure* 3.19:** *Temperature* θ *v/s* Pr

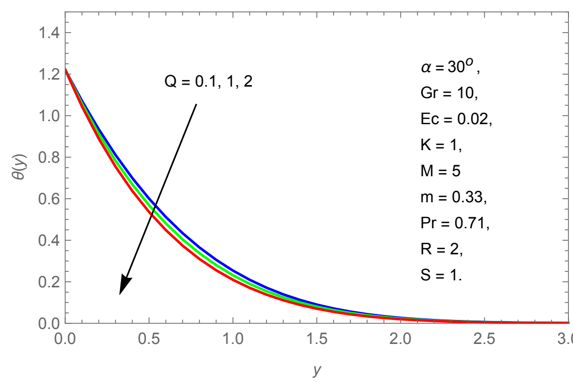

***Figure* 3.20:** *Temperature* θ *v/s* Q

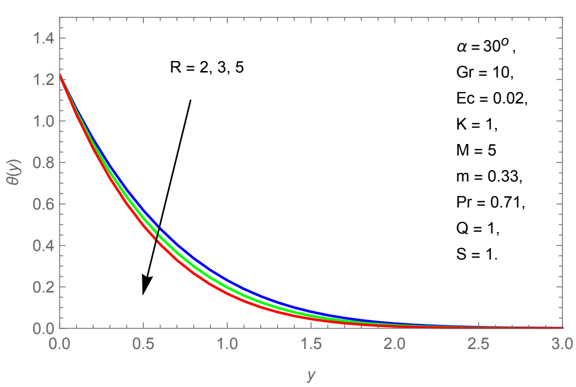

***Figure* 3.21:** *Temperature* θ *v/s* R

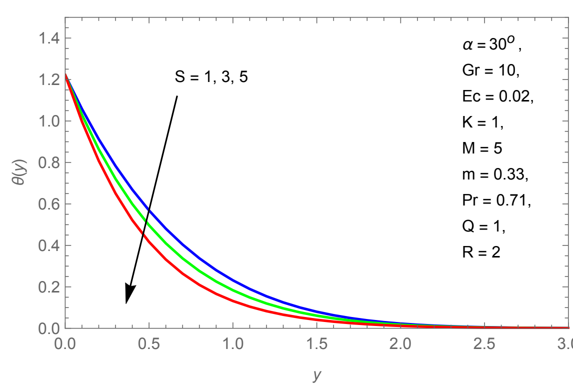

***Figure* 3.22:** *Temperature* θ *v/s* S

Tables 3.1 and 3.2 give the values of skin friction and nusselt number respectively and show how different parameters affect these quantities such as- Based on Table 3.1, skin friction values τ_1 and τ_2 grow in proportion to increases in α, Pr, R, Q, and S. The contrary effect is seen when the figures for K, Gr, and Ec rise. In contrast, the skin frictions are surprisingly affected by m and M; that is, τ_1 decreases and τ_2 increases as m increases but τ_1 increases and τ_2 lowers as M increases. The Nusselt figure for Ec dropped, according to Table 3.2 , but when Pr, R, Q and S were increased, the opposite outcome was seen.

Table 3.1: *Coefficients of skin friction τ_1 and τ_2 for varying parameters value*

α	**K**	**Gr**	**M**	**m**	**Pr**	**R**	**Ec**	**Q**	**S**	τ_1	τ_2
30^0	**1**	**10**	**5**	**0.33**	**0.71**	**2**	**0.02**	**1**	**1**	1.24768	0.507061
45^0	1	10	5	0.33	0.71	2	0.02	1	1	0.900179	0.525578
60^0	1	10	5	0.33	0.71	2	0.02	1	1	0.445472	0.549808
30^0	**0.5**	10	5	0.33	0.71	2	0.02	1	1	1.16679	0.532558
30^0	**5**	10	5	0.33	0.71	2	0.02	1	1	1.31643	0.485516
30^0	1	**5**	5	0.33	0.71	2	0.02	1	1	0.297948	0.557669
30^0	1	**15**	5	0.33	0.71	2	0.02	1	1	2.18847	0.456932
30^0	1	10	**2**	0.33	0.71	2	0.02	1	1	1.52217	0.521526
30^0	1	10	**3**	0.33	0.71	2	0.02	1	1	1.42499	0.514181
30^0	1	10	5	**1.5**	0.71	2	0.02	1	1	1.49436	0.336609
30^0	1	10	5	**3**	0.71	2	0.02	1	1	1.63466	0.385574
30^0	1	10	5	0.33	**1**	2	0.02	1	1	1.06429	0.522542
30^0	1	10	5	0.33	**1.5**	2	0.02	1	1	0.841479	0.53961
30^0	1	10	5	0.33	0.71	**3**	0.02	1	1	1.17182	0.513623
30^0	1	10	5	0.33	0.71	**5**	0.02	1	1	1.1012	0.519531
30^0	1	10	5	0.33	0.71	2	**5**	1	1	1.33266	0.502503
30^0	1	10	5	0.33	0.71	2	**10**	1	1	1.42726	0.497618
30^0	1	10	5	0.33	0.71	2	0.02	**0.1**	1	1.29702	0.50406
30^0	1	10	5	0.33	0.71	2	0.02	**2**	1	1.19637	0.5102
30^0	1	10	5	0.33	0.71	2	0.02	1	**5**	1.15601	0.511781
30^0	1	10	5	0.33	0.71	2	0.02	1	**10**	1.04956	0.517345

Table 3.2: *Nusselt Number coefficients for various parameter values*

Pr	**R**	**Ec**	**Q**	**S**	Nu
0.71	**2**	**0.02**	**1**	**1**	1.63305
1	2	0.02	1	1	1.96001
1.5	2	0.02	1	1	2.43302
0.71	**3**	0.02	1	1	1.76233
0.71	**5**	0.02	1	1	1.89014
0.71	2	**5**	1	1	1.34621
0.71	2	**10**	1	1	0.983352
0.71	2	0.02	**0.1**	1	1.50071
0.71	2	0.02	**2**	1	1.77101
0.71	2	0.02	1	**5**	1.91603
0.71	2	0.02	1	**10**	2.24096

4 Conclusion

This paper investigates radiation effects on thermally stratified fluid with Hall effects, viscous dissipation with heat source/sink and unsteady *MHD* free convectionan incompressible electrically conducting fluid flowing past an inclined plate while a uniform magnetic field is applied. The leading equations are numerically solved by use of the Crank-Nicolson method. The findings show the temperature and velocity as well as other flow properties. Based on the flow analysis, the following findings are made:

- As the angle of inclination α or magnetic parameter M increases, the magnitude of velocity u decreases. The results for the heat absorption parameter Q, radiation parameter R, stratification parameter S and Prandtl number Pr are all the same. With regard to the remaining parameters as the porosity parameter K, hall parameter m, Grashof number Gr and Ekert numbers Ec the opposite conclusions are valid.
  Similar findings apply to velocity w, with the exception of the M, velocity w grows along with M.
- The temperature rises when the Ec rises, whereas the remaining parameters such as Q, R, S and Pr do the reverse.
- As the K, Gr and Ec increase, so does the local skin friction τ_1 and τ_2. As the angle of inclination α, Pr, R, S and Q increase, it also rises. When the M increases, the value of τ_1 rises and τ_2 falls. As the value of m increases, τ_1 declines and τ_2 rises.
- The Nusselt number Nu rises as the Pr, R, Q and S all rise. As the value of the Ec increases, it lowers.

References

[1] R. N. Barik and G. C. Dash, Thermal radiation effect on an unsteady magnetohydrodynamic flow past inclined porous heated plate in the presence of chemical reaction and viscous dissipation, *Applied Mathematics and Computation*, **226** (2014), 423-434.

[2] A. Chakrabarti and A. S. Gupta, Hydromagnetic flow and heat transfer over a stretching sheet, *Quarterly of Applied Mathematics*, **37**(1) (1979), 73-78.

[3] M. K. Choudhary, S. Chaudhary and R. Sharma, Unsteady MHD flow and heat transfer over a stretching permeable surface with suction or injection, *Procedia Engineering*, **127** (2015), 703-710.

[4] A. J. Chamkha, M. Mujtaba, A. Quadri and C. Issa, Thermal radiation effects on *MHD* forced convection flow adjacent to a non-isothermal wedge in the presence of a heat source or sink, *Heat and Mass Transfer*, **39**(4) (2003), 305-312.

[5] S. Das, B. C. Sarkar and R. N. Jana, Hall effect on *MHD* free convection boundary layer flow past a vertical flat plate, *Meccanica*, **48**(6) (2012), 1387-1398.

[6] M. Ferdows, A. A. Afify and E. E. Tzirtzilakis, Hall current and viscous dissipation effects on boundary layer flow of heat transfer past a stretching sheet, *International Journal of Applied and Computational Mathematics*, **3**(4) (2017), 3471-3487.

[7] L. J. Grubka and K. M. Bobba, Heat transfer characteristics of a continuous stretching surface with variable temperature,*Journal of Heat Transfer*, **107**(1) (1985), 248-250.

[8] B. S. Goud, P. Srilatha, D. Mahendar, T. Srinivasulu and Y. Dharmendar Reddy, Thermal radiation effect on thermostatically stratified *MHD* fluid flow through an accelerated vertical porous plate with viscous dissipation impact, *Partial Differential Equations in Applied Mathematics*, **7** (2023), 100488.

[9] D. Iranian, P. Loganathan and P. Ganesan, Unsteady *MHD* natural convective flow over vertical plate in thermally stratified media with variable viscosity and thermal conductivity, *International Journal of Computer Applications*, **121**(3) (2015), 18-24.

[10] S. K. Khan, M. S. Abel and R. M. Sonth, Visco-elastic MHD flow, heat and mass transfer over a porous stretching sheet with dissipation of energy and stress work, *Heat and Mass Transfer*, **40**(1-2) (2003), 47-57.

[11] D. Moalem, Steady state heat transfer within porous medium with temperature dependent heat generation, *International Journal of Heat and Mass Transfer*, **19**(5) (1976), 529-537.

[12] A. M. Megahed and M. G. Reddy, Numerical treatment for *MHD* viscoelastic fluid flow with variable fluid properties and viscous dissipation, *Indian Journal of Physics*, **95**(4) (2020), 673-679.

[13] M. C. Raju, S. V. K. Varma and B. Seshaiah, Heat transfer effects on a viscous dissipative fluid flow past a vertical plate in the presence of induced magnetic field, *Ain Shams Engineering Journal*, **6**(1) (2015), 333-339.

[14] Y. Dharmendar Reddy, B. Shankar Goud and M. Anil Kumar, Radiation and heat absorption effects on an unsteady *MHD* boundary layer flow along an accelerated infinite vertical plate with ramped plate

temperature in the existence of slip condition, *Partial Differential Equations in Applied Mathematics*, **4** (2021), 100166.

[15] S. K. Soid and A. Ishak, Thermal boundary layer flow on a stretching plate with radiation effect, *International Conference on Business, Engineering and Industrial Applications*, 2011.

[16] I. O. Senge, E. O. Oghre and I. F. Ekang, Influence of radiation on magnetohydrodynamics flow over an exponentially stretching sheet embedded in a thermally stratified porous medium in the presence of heat source, *Earthline Journal of Mathematical Sciences,* **5**(2) (2020), 345-363.

[17] E. A. Vijayalakshmi, S. S. Santra, T. Botmart, H. Alotaibi, G. B. Loganathan, M. Kannan, J. Visuvasam and V. Govindan, Analysis of the magnetohydrodynamic flow in a porous medium, *AIMS Mathematics*, **7**(8) (2022), 15182-15194.